Journal of Nuclear Materials 502 (2018) 323–330

Contents lists available at ScienceDirect

Journal of Nuclear Materials

journal homepage: www.elsevier.com/locate/jnucmat

A model describing intra-granular fission gas behaviour in oxide fuel for advanced engineering tools

D. Pizzocri [a], G. Pastore [b], T. Barani [a], A. Magni [a], L. Luzzi [a, *], P. Van Uffelen [c], S.A. Pitts [b], A. Alfonsi [b], J.D. Hales [b]

[a] Politecnico di Milano, Department of Energy, Nuclear Engineering Division, Via La Masa 34, 20156, Milan, Italy
[b] Idaho National Laboratory, P.O. Box 1625, Idaho Falls, ID 83415-3840, United States
[c] European Commission, Joint Research Centre, Directorate for Nuclear Safety and Security, P.O. Box 2340, 76125, Karlsruhe, Germany

HIGHLIGHTS

- Development of a model describing intra-granular fission gas behaviour.
- Physically-based single-size bubble evolution model derived from cluster dynamics.
- Model comparisons to experimental data of bubble radius and number density.
- Uncertainty analysis performed on main model parameters.
- Model in line with the computational requirements for use in fuel performance codes.

ARTICLE INFO

Article history:
Received 24 October 2017
Received in revised form
5 February 2018
Accepted 16 February 2018
Available online 17 February 2018

Keywords:
Fission gas behaviour
Intra-granular behaviour
Oxide fuel
Gaseous swelling
Fuel performance codes

ABSTRACT

The description of intra-granular fission gas behaviour is a fundamental part of any model for the prediction of fission gas release and swelling in nuclear fuel. In this work we present a model describing the evolution of intra-granular fission gas bubbles in terms of bubble number density and average size, coupled to gas release to grain boundaries. The model considers the fundamental processes of single gas atom diffusion, gas bubble nucleation, re-solution and gas atom trapping at bubbles. The model is derived from a detailed cluster dynamics formulation, yet it consists of only three differential equations in its final form; hence, it can be efficiently applied in engineering fuel performance codes while retaining a physical basis. We discuss improvements relative to previous single-size models for intra-granular bubble evolution. We validate the model against experimental data, both in terms of bubble number density and average bubble radius. Lastly, we perform an uncertainty and sensitivity analysis by propagating the uncertainties in the parameters to model results.

1. Introduction

Given the fundamental role played by fission gas swelling and release in the thermo-mechanical behaviour of nuclear fuel rods during irradiation [1,2], models of fission gas behaviour (FGB) must be included in fuel performance codes. Bubbles nucleate in fuel grains due to the low solubility of the fission gas and evolve through trapping of dissolved gas atoms and the counteracting process of irradiation-induced bubble re-solution. Gas diffusion to grain boundaries is mainly due to dissolved atoms, with nucleation, trapping and re-solution determining the coupling between bubble evolution and gas atom diffusion [1–6]. Intra-granular gas diffusion to grain boundaries provides the source term for the inter-granular processes, ultimately leading to grain-boundary gaseous swelling and fission gas release [2,6–8]. Intra-granular bubbles not only affect the gas diffusion rate to grain boundaries but also contribute to fuel swelling, although intra-granular gaseous swelling becomes significant compared to grain-boundary swelling only at high burnup or during transients to high temperatures [9,10].

Therefore, models are needed to describe the evolution of the intra-granular bubble population. In particular, to estimate the bubble effects in intra-granular diffusion and the intra-granular swelling, the bubble number density and average bubble size

* Corresponding author.
E-mail address: lelio.luzzi@polimi.it (L. Luzzi).

https://doi.org/10.1016/j.jnucmat.2018.02.024

need to be calculated [4,11–13].

The traditional approach adopted in engineering-scale fuel performance codes describes the evolution of intra-granular fission gas bubbles by relying on empirical correlations. These correlations estimate the mean bubble size and number density as a function of macroscopic parameters, e.g. the local temperature [6,14]. Indeed, the inherent simplicity of the correlation-based approach entails the advantage of a small computational burden. However, the application of these correlations is limited to their interpolation range, hence to conditions for which experimental data are available. Furthermore, physically based models can be applied to different materials by adapting the fundamental parameters, while empirical correlations are material-specific. Finally, as fundamental parameters can be derived using lower-length scale modelling, physically based engineering models have the additional advantage of allowing for scale bridging in multiscale modelling approaches [15].

A complete and accurate description of the bubble population evolution can be accomplished by employing cluster dynamics approaches (e.g., [16–19]). Cluster dynamics models calculate the entire bubble (atom cluster) size distribution and the distribution evolution over time by solving coupled rate equations for the number densities of clusters of different sizes. Clearly, these advanced modelling approaches are computationally intensive and cannot be used directly for fuel performance code applications [4]. On the other hand, advanced modelling can be used to inform engineering-scale models with improved parameters.

Representing the bubble size distribution as only the mean size and the total number density (single-size models) allows for a compromise between simplicity and accuracy, surpassing the inherent physical limitations of the correlation-based approaches and, at the same time, avoiding the high computational cost of cluster dynamics [4].

The present authors developed an efficient physically based model of fission gas release and swelling in UO_2 [20–22]. This model constitutes the basis for the calculation of fission gas swelling and release in the fuel performance codes TRANSURANUS [11] and BISON [12]. The emphasis of such development has been on modelling of grain-face FGB, while intra-granular behaviour has been modelled in a rather simplistic way and making use of empirical values for the characteristics of the intra-granular bubble population [20,23]. Introducing a more suitable treatment of the intra-granular FGB in this model was identified as an important future development.

In this work, we tackle this task by developing a new model of intra-granular fission gas behaviour that computes the coupled intra-granular bubble evolution and gas atom diffusion on a physical basis. The goal is to compute the evolution during irradiation of intra-granular bubble mean size and number density, the associated intra-granular swelling, and the coupled gas release rate to grain boundaries. A requirement is that the model consists of a reduced number of equations and parameters and can be used in engineering codes directly. Thus, we derive a single-size model from a detailed cluster dynamics description through successive simplifications. These simplifications are corroborated by experimental observations of small intra-granular bubbles, rather than obtained through cluster dynamics simulations. A multiscale approach with comparisons to detailed cluster dynamics simulations in order to assess and potentially improve the assumptions of this engineering-scale model is of interest in perspective, although it is beyond the scope of the present work.

To the best of our knowledge, the most recent and significant work on single-size models for intra-granular bubble evolution is the paper of Olander and Wongsawaeng [4]. They reviewed the mechanisms of bubble nucleation, growth and re-solution and derived single-size formulations by applying in the first place the assumption of all bubbles having the same size. While this approach captures the main physical mechanisms, it has important limitations [4]. For instance, the single-size assumption implies that bubbles nucleated at a given time grow instantaneously to the mean size and that bubble destruction only occurs at the mean size, which introduces a bias in the bubble size calculation. Capturing such effects requires consideration of a non-uniform bubble size distribution. In the present work, we aim to obtain an improvement of this state of the art for single-size models. We start from a detailed cluster dynamics physical representation and derive a formulation for the evolution of the bubble mean size and number density that preserves fundamental size-distribution effects. Moreover, we consider the effect of gas diffusion to grain boundaries coupled to bubble evolution.

In Section 2, we introduce the physical processes that govern the evolution of intra-granular bubbles, i.e., nucleation, re-solution and trapping. In Section 3, we derive a new single-size model suited for oxide fuels starting from the cluster dynamics equations. We validate the model against experimental data (Section 4) and complement the validation with an uncertainty and sensitivity analysis (Section 5). Conclusions are drawn in Section 6.

2. Physical processes

Three fundamental processes control the evolution of small intra-granular bubbles in nuclear fuel, i.e., bubble nucleation, gas atom trapping at the bubbles, and irradiation-induced gas atom re-solution from bubbles back into the lattice. Nucleation can be considered as driven by either diffusion [24,25], or by irradiation [6], while re-solution is (primarily) irradiation-driven [14,26], and trapping is (mainly) diffusion-driven [27]. For an extensive overview of the modelling of these processes, we recommend the work of Olander and Wongsawaeng [4].

We adopt here the terminology of Olander and Wongsawaeng [4] for the different possible mechanisms of nucleation and re-solution, i.e., *heterogeneous* and *homogeneous*. *Heterogeneous* nucleation and re-solution refer to the nuclei of the new bubbles being created as a direct consequence of the interaction of fission fragments with the lattice and the bubbles being destructed *en-bloc* by passing fission fragments, respectively. The *homogeneous* mechanisms refer to bubbles being nucleated by diffusion-driven interactions of dissolved gas atoms and re-solution occurring gradually by ejection of individual atoms. There are several experimental results and theoretical considerations on the *heterogeneous*/*homogeneous* nature of nucleation, re-solution and trapping in oxide fuel. Each of these processes is modelled by introducing a specific rate of event occurrence. Here, we denote the nucleation rate as ν, the re-solution rate as α, and the trapping rate as β.

Focusing first on nucleation, several TEM observations show intra-granular bubbles lying in straight lines [4,9,28]. Turnbull's early conclusion was that bubbles were nucleated *heterogeneously* along the track of fission fragments, with nucleation being driven directly by irradiation [29]. Nevertheless, several further observations did not show aligned bubbles, thus hindering the generality of such conclusion [4], [30]. Additionally, the typical thickness of TEM samples is lower than the range of fission fragments, therefore only portions of actual fission tracks are observed [4]. The other nucleation mechanism, which competes with the *heterogeneous* mechanism, is the *homogeneous*, diffusion-controlled production of dimers (diatomic fission gas clusters) [24,25]. Presumably, both these mechanisms are active and competing in the fuel grains, but major experimental and theoretical works agree on the dominance of the *heterogeneous* mechanism [29–31]. Then, in this work we assume that the *heterogeneous* nucleation mechanism is dominant

in oxide fuels. The expression for the nucleation rate is thus

$$\nu = 2\eta F \tag{1}$$

where ν (nucleated bubbles m^{-3} s^{-1}) is the nucleation rate, η (nucleated bubbles per fission fragment) is a number generally considered in the range 5–25 based on experimental observations [29,30], F is the fission rate density (fissions m^{-3} s^{-1}), and the factor 2 accounts for the number of fission fragments per fission. The use of this expression for the nucleation rate underlies the assumption of bubbles being formed in the wake of fission fragments (with the creation of vacancy clusters that are rapidly filled by gas atoms). Clearly, this is a simplified representation of the nucleation mechanism, consistent with the overall modelling approach.

As for re-solution, we also assume a dominating *heterogeneous* mechanism. The re-solution rate is expressed as proportional to the fission rate density [6,14,29],

$$\alpha = 2\pi\mu_{ff}\left(R + R_{ff}\right)^2 F \tag{2}$$

where α (re-solved bubbles $bubble^{-1}$ s^{-1}) is the re-solution rate, μ_{ff} (m) and R_{ff} (m) are the average length and radius of a fission spike (the subscript ff corresponds to fission fragment), respectively, and R (m) is the radius of the gas bubble. The assumption of *heterogeneous* re-solution of small intra-granular bubbles is supported by the molecular dynamics work performed by Govers et al. [32]. They investigated both the *homogeneous* re-solution mechanism (as originally described by Nelson [33]) and the *heterogeneous* mechanism (originally proposed by Turnbull [29] and in agreement with other contemporary work [34,35]). Their analysis demonstrated that the *heterogeneous* re-solution mechanism is more effective in re-solving fission gas bubbles compared to the *homogeneous* mechanism. However, they showed that for a wide variety of bubble radii and gas densities, no clear dependence of the re-solution rate on the bubble size emerges [32]. Other combined Monte Carlo and molecular dynamics approaches indicated the predominance of the *homogeneous* re-solution mechanism [36–38]. Further molecular dynamics work could shed further light on the mechanisms of re-solution and enable a more accurate consideration of the re-solution rate, which in perspective can be incorporated in the present model by replacing Eq. (2).

As for the trapping rate, following the formulation derived by Ham [27], we write

$$\beta = 4\pi D(R + R_{at})c_1 \tag{3}$$

where β (trapped atoms $bubble^{-1}$ s^{-1}) is the trapping rate, D (m^2 s^{-1}) is the diffusion coefficient of single gas atoms, R (m) is the radius of a bubble, R_{at} (m) is the radius of a single gas atom in the lattice, and c_1 (atoms m^{-3}) is the concentration of single gas atoms. These three rate equations (Eqs. (1)–(3)) are used in the present intra-granular gas behaviour model for computing the bubble nucleation, re-solution and gas atom trapping rates.

3. Model derivation

We present here a model to describe the intra-granular gas behaviour. This results from the combination of the intra-granular bubble population evolution, through the physical processes described in Section 2, and the gas diffusion towards grain boundaries.

Following the assumptions of Clement and Wood [39] and Fell and Murphy [40], we limit our scope to clusters made of only gas atoms and neglect vacancy absorption at the clusters. This assumption is in line with the observation that because of the small size of intra-granular bubbles, the surface-tension force is large enough to keep the gas density near that of solid xenon [4]. Several experimental observations of over-pressurized intra-granular bubbles corroborate this assumption [9,14,29,30,41]. The assumption of single-species (i.e., atoms-only) cluster dynamics implies that the gas atoms are considered to completely occupy available vacancies.

Consistent with this approach, and in line with [4], we adopt the assumption of the gas density in the bubbles being constant. It follows that the radius of a bubble containing n gas atoms is calculated as

$$R_n = Bn^{1/3} \tag{4}$$

where $B = (3\Omega/4\pi)^{1/3}$ with Ω being the atomic volume. Olander and Wongsawaeng [4] adopted a value of $\sim 7\cdot10^3$ kg m^{-3} for the gas density in bubbles with radii of 0.5–2 nm, based on extrapolation of the gas density data for larger bubbles from Refs. [44,45]. However, this value corresponds to an atomic volume of $\sim 3\cdot10^{-29}$ m^3, which is lower than the volume of the Schottky defect. Moreover, the interpolation of the data from Refs. [44,45], rather suggests a density value around $5\cdot10^3$ kg m^{-3}. In this work, we consider an atomic volume in the bubbles of $\Omega = 4.09\cdot10^{-29}$ m^3, i.e., equal to the volume of the Schottky defect [46]. Choosing the atomic volume as equal to the volume of the Schottky defect is consistent with the assumption that the gas atoms in the bubbles completely occupy available vacancies. Furthermore, this value for the atomic volume corresponds to a gas density of $\sim 5.4\cdot10^3$ kg m^{-3}, which is consistent with the available experimental evidence, as discussed above.

Clearly, the hypothesis of constant gas density in the bubbles is not meant to be fully representative of the underlying physics, and a more detailed approach would involve the use of an equation of state. Confirming this modelling assumption by performing two-species (gas atoms and vacancies) cluster dynamics analyses is of interest in perspective.

In the cluster dynamics model, a cluster is defined by its size (the number of gas atoms contained within the cluster) and the number density for each species of clusters is governed by a partial differential equation. We write the master equations of cluster dynamics considering that (a) the processes of cluster evolution occur at the rates described in Section 2, and (b) the nucleation and re-solution processes are *heterogeneous*. For the sake of clarity, Fig. 1 depicts the processes of cluster evolution for the first three cluster sizes (single atoms, dimers and trimers). The master equations of the cluster dynamics model are

$$\begin{cases} \dfrac{\partial c_1}{\partial t} = +yF + D\nabla^2 c_1 - 2\nu - \displaystyle\sum_{n=2}^{\infty}\beta_n c_n + \sum_{n=2}^{\infty} n\alpha_n c_n \\ \dfrac{\partial c_2}{\partial t} = +\nu - (\beta_2 + \alpha_2)c_2 \\ \vdots \\ \dfrac{\partial c_n}{\partial t} = +\beta_{n-1}c_{n-1} - (\beta_n + \alpha_n)c_n \end{cases} \tag{5}$$

where c_1 (atoms m^{-3}) is the concentration of single gas atoms, and c_2, c_3, …, c_n (clusters m^{-3}) are the number densities of clusters of atomic size 2, 3, …, n, respectively. Other than the fission yield y (atoms $fiss^{-1}$), the other quantities in Eqs. (5) have been defined in Section 2.

We include the diffusion term only for single gas atoms, assuming that larger clusters (bubbles) are immobile [26,30]. On the same basis, we neglect interactions between clusters (bubble coalescence). The assumption of immobile bubbles may be not

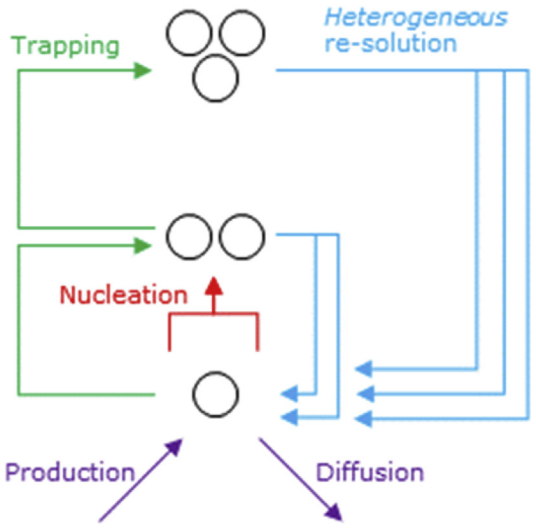

Fig. 1. Sketch of the mechanisms of cluster dynamics. Nucleation is assumed to create only dimers ($n = 2$). *Heterogeneous* re-solution destroys entire bubbles, transferring n atoms from the bubble to the single gas atoms bin. We consider production (from fission reactions) and diffusion to affect only single gas atoms.

valid at high temperatures above 1500–1800 °C [9,14,42,43]. Note that we assume that bubbles nucleate as dimers. If nucleation is heterogeneous, it is possible that the size of the nucleated bubbles depends upon the concentration of dissolved gas [4], hence this is an arbitrary assumption.

The simultaneous solution of Eqs. (5) provides the complete cluster size distribution. Nevertheless, Eqs. (5) define a system of a large number (thousands) of coupled differential equations whose solution is impractical for direct application to engineering codes, both in terms of computational cost and memory requirement, even with the application of grouping schemes [4,40]. In order to reduce the dimension of the cluster dynamics system, we introduce two broader cluster categories, i.e., clusters of size $n = 1$ (single atoms) and clusters of size $n > 1$ (bubbles). We define the number density of bubbles, N (bubbles m^{-3}), and the total concentration of gas in bubbles, m (atoms m^{-3}), as

$$N = \sum_{n=2}^{\infty} c_n \tag{6}$$

$$m = \sum_{n=2}^{\infty} n c_n \tag{7}$$

Combining Eqs. (6) and (7) with the cluster dynamics master equations (Eqs. (5)), we obtain a system of three partial differential equations

$$\begin{aligned}
\frac{\partial N}{\partial t} &= +\nu - \sum_{n=2}^{\infty} \alpha_n c_n \\
\frac{\partial m}{\partial t} &= +2\nu + \sum_{n=2}^{\infty} \beta_n c_n - \sum_{n=2}^{\infty} n \alpha_n c_n \\
\frac{\partial c_1}{\partial t} &= +yF + D\nabla^2 c_1 - 2\nu - \sum_{n=2}^{\infty} \beta_n c_n + \sum_{n=2}^{\infty} n \alpha_n c_n
\end{aligned} \tag{8}$$

The series in Eq. (8) can be approximated by applying the Taylor expansion of $\alpha_n = \alpha(n)$ and $\beta_n = \beta(n)$ in conjunction with the definitions given in Eqs. (6) and (7). For the re-solution rate defined by Eq. (2) and making use of the assumption defined by Eq. (4), we obtain

$$\begin{aligned}
\alpha_n &= \alpha_{\overline{n}} + \left[\frac{d\alpha_n}{dn}\right]_{\overline{n}} (n - \overline{n}) + o(n - \overline{n}) \\
&\approx \alpha_{\overline{n}} \left(1 + \frac{2}{3} \frac{B n \overline{n}^{-2/3} - B \overline{n}^{1/3}}{B \overline{n}^{1/3} + R_{\mathrm{ff}}}\right) = \alpha_{\overline{n}} \varphi_{n,\overline{n}} \approx \alpha_{\overline{n}}
\end{aligned} \tag{9}$$

For the trapping rate defined by Eq. (3), considering that it is proportional to the bubble radius and again making use of the assumption defined by Eq. (4), we obtain

$$\begin{aligned}
\beta_n &= \beta_{\overline{n}} + \left[\frac{d\beta_n}{dn}\right]_{\overline{n}} (n - \overline{n}) + o(n - \overline{n}) \approx \beta_{\overline{n}} \left(\frac{2}{3} + \frac{1}{3} \frac{n}{\overline{n}}\right) \\
&= \beta_{\overline{n}} \psi_{n,\overline{n}} \approx \beta_{\overline{n}}
\end{aligned} \tag{10}$$

The final approximate equalities in Eqs. (9) and (10) are based on the coefficients $\varphi_{n,\overline{n}}$ and $\psi_{n,\overline{n}}$ being close to unity for a size distribution that peaks near the average value. This kind of size distribution is typical of experimental observations of intra-granular bubbles [29,30]. It is of interest in perspective to confirm or refine this assumption based on comparison to detailed cluster dynamics simulations considering the full-size distribution of intra-granular bubbles, although this is out of the scope of the present work. It is worth noting that it is possible to refine the approximation in our model by including more terms in the Taylor expansions.

With the approximations of Eqs. (9) and (10) and the definitions given in Eqs. (6) and (7), Eq. (8) become

$$\begin{aligned}
\frac{\partial N}{\partial t} &= +\nu - \alpha_{\overline{n}} N \\
\frac{\partial m}{\partial t} &= +2\nu + \beta_{\overline{n}} N - \alpha_{\overline{n}} m \\
\frac{\partial c_1}{\partial t} &= +yF + D\nabla^2 c_1 - 2\nu - \beta_{\overline{n}} N + \alpha_{\overline{n}} m
\end{aligned} \tag{11}$$

We close the system by defining the average number of atoms in a bubble and the average bubble radius, respectively, as

$$\begin{aligned}
\overline{n} &= m/N \\
R_{\overline{n}} &= B \overline{n}^{1/3}
\end{aligned} \tag{12}$$

For spherical bubbles, the swelling component due to intra-granular bubbles is at last

$$\left(\frac{\Delta V}{V}\right)_{ig} = \frac{4}{3} \pi R_{\overline{n}}^3 N \tag{13}$$

Note that the total intra-granular swelling is given by the sum of the contributions due to bubbles and dissolved fission products. Eq. (13) only accounts for swelling due to fission gas bubbles. As atoms are transferred from the solution to the bubbles, the matrix swelling due to dissolved fission gas decreases correspondingly. Also, the matrix swelling due to other fission products is operational [24].

The final formulation of the model, Eqs. (11)–(13), leads to a number of considerations. The bubble number density, N, varies according to the rate of nucleation of new bubbles and the re-solution rate, with the latter corresponding to the bubble destruction rate in the heterogeneous interpretation. Note that the derivation from the equations of cluster dynamics leads to the same rate equation for the total bubble number density in the heterogeneous model of Olander and Wongsawaeng [4]. Rather than by starting from the detailed physical description of cluster dynamics, the model in Ref. [4] was derived by applying in the first place the assumption of all bubbles having the same size and, consistently, of

Table 1
List of model parameters.

Symbol	Definition	Value	u.o.m.	Reference
η	Number of bubbles nucleated per fission fragment	25	bubbles ff^{-1}	[6]
μ_{ff}	Range of a fission fragment in UO_2	6	μm	[4,6]
R_{ff}	Radius of influence of a fission fragment track	1	nm	[4,6]
D	Diffusion coefficient of fission gas in UO_2 $D_1 + D_2 + D_3$ $D_1 = 7.6\cdot10^{-10}\exp(-4.86\cdot10^{-19}/kT)$ $D_2 = 4\cdot1.41\cdot10^{-25}\sqrt{F}\exp(-1.91\cdot10^{-19}/kT)$ $D_3 = 2\cdot10^{-40}F$		m^2 s^{-1}	[28]
R_{at}	Radius of a gas atom in the lattice	0.2	nm	Estimate, [4]
Ω	Atomic gas volume in bubbles	$4.09\cdot10^{-2}$	nm^3	[46]

the re-solution and trapping rate being the same for all bubbles. The calculation of the average number of atoms in a bubble, $\bar{n}$, differs from the heterogeneous model of Olander and Wongsawaeng [4] in that it naturally includes the effects of nucleation and re-solution through the equations for m and N , Eq. (11). In particular, nucleation and re-solution affect the average bubble size because in general bubbles are created/destructed at sizes different from the mean. These effects can be considered only if a size distribution of bubbles is considered and cannot be naturally included through a pure single-size derivation. Our model based on the detailed cluster dynamics approach introduces these important bubble-distribution related effects in a formulation that in its final form only includes equations for the average quantities. In Ref. [4], this problem is circumvented by introducing the effects of nucleation and re-solution on the average bubble size *a posteriori* through consideration of the average bubble lifetime.

Furthermore, the present model overcomes the assumption in Ref. [4] of gas diffusion to grain boundaries being neglected. Eqs. (11)–(13) describe intra-granular gas behaviour in terms of bubble evolution coupled to gas diffusion. We solve the set of coupled differential equations to calculate both intra-granular bubble swelling and fission gas release to grain boundaries. The diffusion equation is solved numerically using a recently developed algorithm [47].

The new model is a description of intra-granular bubble evolution coupled to diffusion that depends on a reduced number of equations and parameters, and can be applied directly to engineering codes. The procedure applied to derive the formulation drastically reduces model complexity relative to the reference cluster dynamics model, while retaining important physical details that are associated with the presence of a non-uniform bubble size distribution and are therefore inherent in the cluster dynamics model, but not fully compatible with traditional single-size approaches.

4. Model comparisons to experimental data

In this section, we perform initial comparisons of the present model to experimental data. The reference values for each model parameter are collected in Table 1. All the calculations are performed with the model implemented as a stand-alone computer code.

The available experimental databases for intra-granular bubble size and number density as a function of well-defined irradiation conditions and also considered for experimental comparisons by Olander and Wongsawaeng [4] include the data from Baker [30] and Kashibe et al. [9]. In this work we excluded the data from Kashibe et al., [9], because they involved a significant coarsening of the bubbles occurring at high burnup. Modelling intra-granular bubble coarsening requires considering additional bubble growth mechanisms to those governing the evolution of smaller bubbles. Such mechanisms are not yet fully understood, but plausibly involve significant vacancy absorption at the bubbles and/or bubble coalescence [9,48,49], which the present model does not represent. The extension of the model to bubble coarsening is out of the scope of this work, however, it is of interest in perspective.

The data from Baker [30] consist of nine measurements of average bubble size and bubble number density. These measurements were performed on samples irradiated at various temperatures (from 1273 to 2073 K) up to a burnup of 23 GWd t^{-1}. In our simulations, to reproduce fuel irradiation up to this burnup we assume a typical fission rate density $F = 1\cdot10^{19}$ fiss m^{-3} s^{-1} kept constant for an irradiation time of 5500 h.

Fig. 2 shows the results of our model in comparison with the experimental data. Results are provided both in terms of average bubble radius and bubble number density. We introduce a non-dimensional validation metric, q, defined as the logarithm of the ratio between a simulation result y_i and the corresponding experimental data x_i, i.e.

$$q = \mathrm{Log}\left(\frac{y_i}{x_i}\right) \tag{14}$$

This validation metric is zero for $y_i = x_i$, whereas values of $q = \pm1, 2, \ldots$correspond to one, two, …order of magnitude difference between simulation results and experimental data. The simulation results (obtained with the model parameters listed in Table 1), the experimental data and the relative values for the validation metric are collected in Tables 2 and 3 for the bubble radius and number density, respectively. Overall, a good agreement between the simulation results and the experimental data is observed. The average values of q over the entire database are −0.06 and −0.11 for the bubble radius and number density, respectively.

5. Uncertainty and sensitivity analysis

We performed an uncertainty analysis of the model to the nucleation rate (Eq. (1)), the re-solution rate (Eq. (2)), and the trapping rate (Eq. (3)). The purpose of this uncertainty analysis is to provide an indication of the propagation of uncertainties from the fundamental model parameters to the model results. We choose to limit the uncertainty analysis to the three rates described in Section 2. We randomly sampled scaling factors for the model parameters within ranges representative of the uncertainties associated with these rates (see Eqs (1)–(3)). In particular, for the nucleation rate we use scaling factors in the range $[0.2, 1]$. This range is justified by several experimental observations reporting 5 to 25 bubbles per fission track [29,30]. As for the re-solution rate, we use scaling

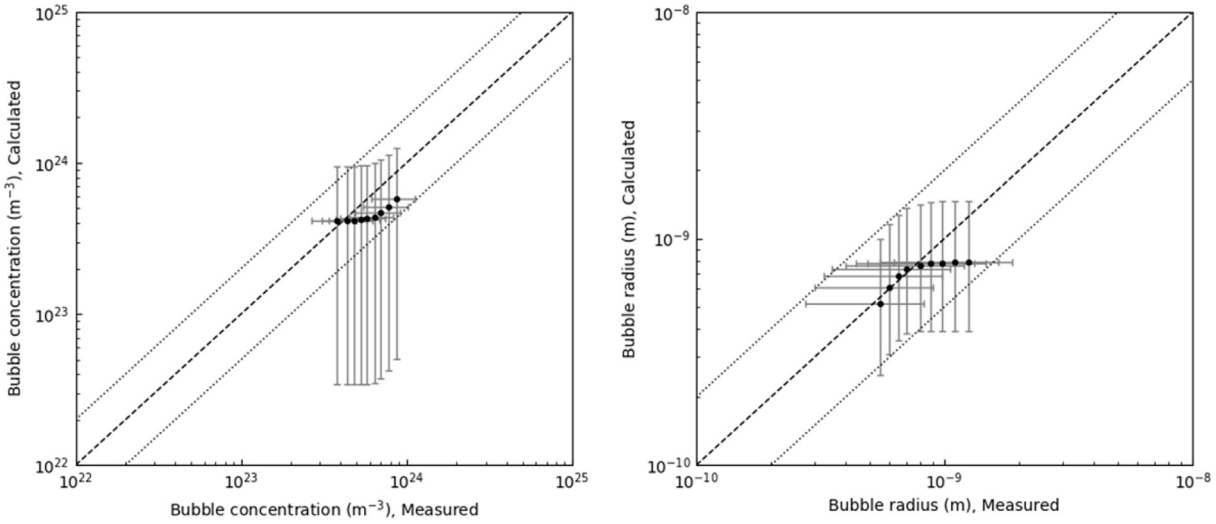

Fig. 2. Comparison between the present model results and the data from Baker [30]. Each full symbol represents a simulation obtained with the reference model parameters compared to the corresponding experimental value. The vertical error bars span the maximum and minimum results obtained in the 2000 simulations performed for each experimental case. The horizontal error bars represent the experimental uncertainties, i.e., 30% for the bubble number density and 50% for the bubble radius [9,30]. The distance from the 45° dashed black line is a graphical measure of accuracy. The dashed grey lines correspond to deviations of a factor of 2 from measured data.

Table 2
Intra-granular bubble radius (nm) simulation results compared to Baker data [30]. The results of Olander and Wongsawaeng's model, taken from Ref. [4], are reported for additional comparison.

Temperature (K)	Exp. [30]	Olander and Wongsawaeng [4]		Present model	Validation metric[a]
		Heterogeneous	*Homogeneous*		
1273	0.55	0.4	1.0	0.515	−0.03
1373	0.60	–	–	0.607	0.005
1473	0.65	–	–	0.681	0.02
1573	0.70	–	–	0.733	0.02
1673	0.80	–	–	0.763	−0.02
1773	0.88	–	–	0.776	−0.05
1873	0.98	1.6	5.1	0.782	−0.096
1973	1.10	–	–	0.784	−0.15
2073	1.25	–	–	0.785	−0.20

[a] The validation metric adopted in this work is defined as Log(calculated value/experimental value) (Eq. (14)). For brevity, we report only the values of this metric for the results of the present model.

Table 3
Intra-granular bubble number density (10^{23} bubbles m^{-3}) simulation results compared to Baker data [30]. The results of Olander and Wongsawaeng's model, taken from Ref. [4], are reported for additional comparison.

Temperature (K)	Exp. [30]	Olander and Wongsawaeng [4]		Present model	Validation metric[a]
		Heterogeneous	Homogeneous		
1273	8.7	7	3	5.78	−0.18
1373	7.8	–	–	5.14	−0.18
1473	7.0	–	–	4.69	−0.17
1573	6.4	–	–	4.42	−0.16
1673	5.7	–	–	4.27	−0.13
1773	5.3	–	–	4.20	−0.10
1873	4.8	2	0.03	4.18	−0.06
1973	4.4	–	–	4.17	−0.02
2073	3.8	–	–	4.17	0.04

[a] The validation metric adopted in this work is defined as Log(calculated value/experimental value) (Eq. (14)). For brevity, we report only the values of this metric for the results of the present model.

[1] This range is lower than the range [0.1, 10] used by Pastore et al. for their uncertainty analysis work [21]. Nevertheless, the wider range proposed by Pastore et al. is meant to account also for the difference in the parameters according to different interpretations of the process, i.e., *heterogeneous* and *homogenous* re-solution [21], whereas in this work we consider one mechanism only and assume pure *heterogeneous* re-solution (Section 2). Under this assumption, reducing the uncertainty from a factor of ten to a factor of two is deemed appropriate.

factors in the range[0.5, 2][1]. The range we use for the trapping rate scaling factors is [0.2, 5]. This range mainly reflects the experimental uncertainty on the diffusion coefficient [28,43]. For each one of the nine experimental data points from Baker [30] we performed 2000 simulations with random sampling of the scaling factors, i.e., we adopted a Monte Carlo approach. Fig. 2 summarizes

the results of this uncertainty analysis, showing the range of variation of the model results associated with the variation of the model parameters, for both the bubble number density and the bubble radius. We also include the experimental uncertainty associated with the data. Note that the resulting uncertainty associated with the predicted bubble radius is comparable to the experimental one (Fig. 2). The accurate calculation of the bubble radius is of particular relevance because the bubble radius affects the intra-granular bubble swelling with a power of three, compared to a power of one for the bubble number density (Eq. (13)).

In order to investigate the sensitivities of the model to each of the uncertain parameters used in the uncertainty analysis (nucleation, re-solution, and trapping rates), we performed a sensitivity analysis. We considered the same variation range for the parameters as in the uncertainty analysis above, and the intra-granular bubble swelling as the figure of merit for the sensitivity analysis. The results are collected in Fig. 3, in terms of Pearson coefficients and normalized sensitivity coefficients as a function of the temperature. Both the Pearson coefficients and the normalized sensitivity coefficients are monotonically varying with temperature, and no strong dependence of the relative importance of the parameters on the temperature is observed. The results indicate that the trapping rate is the dominant parameter over the entire temperature range considered (with respect to the intra-granular bubble swelling). Because the uncertainty range used for the trapping rate mainly reflects the uncertainties in the gas atom diffusion coefficient, (Eq. (3)), such a result confirms the importance of the uncertainty in this model parameter.

6. Conclusions

In this work, we developed a model for the description of the intra-granular behaviour of fission gas in oxide fuel. In particular, the model computes the evolution of intra-granular bubble number density and size coupled to intra-granular gas atom diffusion to grain boundaries. The developed model finds its foundations in cluster dynamics but provides a single-size representation of the bubble distribution. As opposed to previous single-size models for intra-granular bubble evolution, our derivation from the detailed cluster dynamics description leads to consideration of important effects related to the presence of a non-uniform bubble size distribution. This advantage comes at no cost in terms of additional model complexity since the final formulation includes only three coupled differential equations for the bubble mean size, number density, and the concentration of dissolved gas. Therefore, this model can be efficiently used in fuel performance codes. To summarize, the main outcomes of the work are:

- The derivation of a new physically based single-size model starting from the detailed equations of cluster dynamics.
- The validation as a stand-alone code against experimental measurements in a wide temperature range shows a good predictive capability, both in terms of bubble number density and average bubble radius.
- The uncertainty analysis performed with respect to the model parameters (nucleation rate, re-solution rate, and trapping rate) complements the validation, quantifying the impact of the uncertainties in the model parameters on the model results.
- The sensitivity analysis highlights the importance of the trapping rate (hence, of the gas atom diffusion coefficient) over the other parameters in the temperature range of interest for the experiments considered.

Being largely based on theory rather than empirical relations, the new model provides a basis for future developments and for scale bridging in a potential multiscale modelling approach. In this respect, using detailed cluster dynamics calculations as well as atomistic calculations to inform the present engineering-scale model with improved parameters is of interest. Such future work may also include two-species (atoms, vacancies) cluster dynamics calculations to obtain improved information on the gas density in intra-granular bubbles.

The new model can also be applied to fuel materials other than UO_2 by adapting the model parameters. Potential future applications include mixed oxide (MOX) fuels. Also, because the model can be informed by fundamental parameters extracted at the lower-length scale with advanced modelling techniques, it is potentially transferable to new fuel materials for which experimental data are unavailable. Moreover, with an analogous derivation a model can be obtained that considers *homogeneous* nucleation/re-solution mechanisms. This may add generality to the developed approach as potentially applicable to fuel types characterized by a different

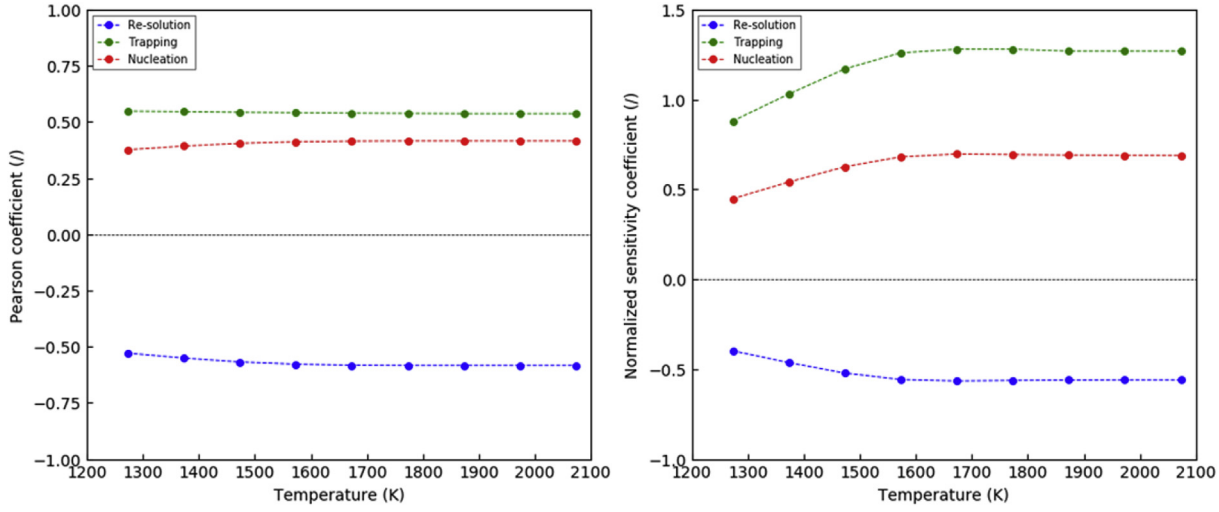

Fig. 3. Results of the sensitivity analysis performed on the re-solution, trapping and nucleation rates, using the intra-granular bubble swelling as the figure of merit. The results are shown in terms of Pearson coefficients (left) and normalized sensitivity coefficients (right), as a function of temperature. The trapping rate is the dominant model parameter over the considered temperature range.

nature of the nucleation/re-solution mechanisms.

Finally, the model does not consider yet the rapid growth of a second population of larger bubbles (tens to hundreds of nm) observed at high burnup or during transients to high temperatures, known as intra-granular bubble coarsening. Model extension to bubble coarsening is of interest in perspective.

Acknowledgments

This research has received funding from the U.S. Department of Energy, Office of Nuclear Energy through the Scientific Discovery through Advanced Computing (SciDAC) project on Fission Gas Behaviour under Award No. DE-SC0016464, and from the Euratom research and training programme 2014–2018 through the INSPYRE project under Grant Agreement No. 754329.

This research contributes to the Joint Programme on Nuclear Materials (JPNM) of the European Energy Research Alliance (EERA), in the specific framework of the COMBATFUEL Project. The work is also part of the R&D activities carried out by Politecnico di Milano in the framework of the IAEA Coordinated Research Project FUMAC (CRP-T12028, Fuel Modelling in Accident Conditions). Finally, the work contributes to the U.S.-EURATOM International Nuclear Energy Research Initiative (INERI) project 2017-004-E on Modelling of Fission Gas Behaviour in Uranium Oxide Nuclear Fuel Applied to Engineering Fuel Performance Codes.

The submitted manuscript has been authored by a contractor of the U.S. Government under Contract DE-AC07-05ID14517. Accordingly, the U.S. Government retains a non-exclusive, royalty free license to publish or reproduce the published form of this contribution, or allow others to do so, for U.S. Government purposes.

References

[1] D.R. Olander, Fundamental Aspects of Nuclear Reactor Fuel Elements Fundamental Aspects of Nuclear Reactor Fuel Elements, 1976.
[2] P. Van Uffelen, R.J.M. Konings, C. Vitanza, J. Tulenko, Analysis of reactor fuel rod behavior, in: D.G. Cacuci (Ed.), Handbook of Nuclear Engineering, Springer Science + Business Media, LLC, New York, NY, USA, 2010, pp. 1519–1627.
[3] H. Matzke, Gas release mechanisms in UO_2 - a critical review, Radiat. Eff. 53 (1980) 219–242.
[4] D.R. Olander, D. Wongsawaeng, Re-solution of fission gas - a review: Part I. Intragranular bubbles, J. Nucl. Mater. 354 (no. 1–3) (2006) 94–109.
[5] M.V. Speight, A calculation on the migration of fission gas in material exhibiting precipitation and Re-solution of gas atoms under irradiation, Nucl. Sci. Eng. 37 (1969) 180–185.
[6] R.J. White, M.O. Tucker, A new fission gas release model, J. Nucl. Mater. 118 (1) (1983) 1–38.
[7] D.R. Olander, Theory of helium dissolution in uranium dioxide. II. Helium solubility, J. Chem. Phys. 43 (3) (1965) 785–788.
[8] R.J. White, The development of grain-face porosity in irradiated oxide fuel, J. Nucl. Mater. 325 (1) (2004) 61–77.
[9] S. Kashibe, K. Une, K. Nogita, Formation and growth of intragranular fuels with burnup of 6-83 GWd/t fission gas bubbles in UO_2, J. Nucl. Mater. 206 (1993) 22–34.
[10] R.J. White, R.C. Corcoran, P.J. Barnes, A Summary of Swelling Data Obtained from the AGR/Halden Ramp Test Programme, 2006.
[11] K. Lassmann, A. Schubert, P. Van Uffelen, C. Gyori, J. van de Laar, TRANSURANUS Handbook, Copyright © 1975-2014, Institute for Transuranium Elements, Karlsruhe, Germany, 2014.
[12] J.D. Hales, et al., BISON Theory Manual: the Equations behind Nuclear Fuel Analysis, 2014. Tech. Rep. INL/EXT-13–29930, Rev. 1, Idaho Falls, ID, USA.
[13] L. Noirot, MARGARET: a comprehensive code for the description of fission gas behavior, Nucl. Eng. Des. 241 (6) (2011) 2099–2118.
[14] P. Lösönen, On the behaviour of intragranular fission gas in UO_2 fuel, J. Nucl. Mater. 280 (1) (2000) 56–72.
[15] T.M. Besmann, State-of-the-Art Report on Multi-scale Modelling of Nuclear Fuels, 2015 no. NEA/NSC/R/(2015)5.
[16] J. Rest, A. Zawadski, FASTGRASS : a Mechanistic Model for the Prediction of Xe, I, Cs, Te, Ba, and Sr Release from Nuclear Fuel under Normal and Severe-accident Conditions, 1993. Report NUREG/CR-5840, ANL-92/3.
[17] M.P. Surh, J.B. Sturgeon, W.G. Wolfer, Master equation and Fokker-Plack methods for void nucleation and growth in irradiation swelling, J. Nucl. Mater. 325 (2004) 44–52.
[18] M. Freyss, Multiscale modelling of nuclear fuels under irradiation, in: EPJ Web of Conferences, 2013.
[19] S. Maillard, R. Skorek, P. Maugis, M. Dumont, Rate theory, in: NEA/NSC/R(2015)5, 2015, pp. 300–308.
[20] G. Pastore, L. Luzzi, V. Di Marcello, P. Van Uffelen, Physics-based modelling of fission gas swelling and release in UO_2 applied to integral fuel rod analysis, Nucl. Eng. Des. 256 (2013) 75–86.
[21] G. Pastore, et al., Uncertainty and sensitivity analysis of fission gas behavior in engineering-scale fuel modeling, J. Nucl. Mater. 456 (2015) 398–408.
[22] T. Barani, et al., Analysis of transient fission gas behaviour in oxide fuel using BISON and TRANSURANUS, J. Nucl. Mater. 486 (2017) 96–110.
[23] M.R. Tonks, et al., Development of a multiscale thermal conductivity model for fission gas in UO_2, J. Nucl. Mater. 469 (2016) 89–98.
[24] J. Spino, J. Rest, W. Goll, C.T. Walker, Matrix swelling rate and cavity volume balance of UO_2 fuels at high burn-up, J. Nucl. Mater. 346 (no. 2–3) (2005) 131–144.
[25] M.S. Veshchunov, On the theory of fission gas bubble evolution in irradiated UO 2 fuel, J. Nucl. Mater. 277 (2000).
[26] G. Martin, et al., A NRA study of temperature and heavy ion irradiation effects on helium migration in sintered uranium dioxide, J. Nucl. Mater. 357 (no. 1–3) (2006) 198–205.
[27] F.S. Ham, Theory of diffusion-limited precipitation, J. Phys. Chem. Solid. 6 (4) (1958) 335–351.
[28] J. Turnbull, R. White, C. Wise, The diffusion coefficient for fission gas atoms in uranium dioxide, in: Proc. of Technical Committee Meeting on Water Reactor Fuel Element Computer Modelling in Steady State, Transient and Accidental Conditions, Preston, England, 1988.
[29] J.A. Turnbull, The distribution of intragranular fission gas bubbles in UO_2 during irradiation, J. Nucl. Mater. 38 (2) (1971) 203–212.
[30] C. Baker, The fission gas bubble distribution in uranium dioxide from high temperature irradiated SGHWR fuel pins, J. Nucl. Mater. 66 (1977) 283–291.
[31] G. Martin, et al., Irradiation-induced heterogeneous nucleation in uranium dioxide, Phys. Lett. Sect. A Gen. At. Solid State Phys. 374 (30) (2010) 3038–3041.
[32] K. Govers, C.L. Bishop, D.C. Parfitt, S.E. Lemehov, M. Verwerft, R.W. Grimes, Molecular dynamics study of Xe bubble re-solution in UO_2, J. Nucl. Mater. 420 (no. 1–3) (2012) 282–290.
[33] R.S. Nelson, The stability of gas bubbles in an irradiation environment, J. Nucl. Mater. 31 (2) (1969) 153–161.
[34] A.D. Whapham, Electron microscope observation of the fission-gas bubble distribution in UO_2, Nucl. Technol. 2 (2) (1966) 123–130.
[35] H. Blank, H. Matzke, The effect of fission spikes on fission gas re-solution, Radiat. Eff. 17 (1973).
[36] D. Schwen, M. Huang, P. Bellon, R.S. Averback, Molecular dynamics simulation of intragranular Xe bubble re-solution in UO_2, J. Nucl. Mater. 392 (1) (2009) 35–39.
[37] M. Huang, D. Schwen, R.S. Averback, Molecular dynamic simulation of fission fragment induced thermal spikes in UO_2: sputtering and bubble re-solution, J. Nucl. Mater. 399 (no. 2–3) (2010) 175–180.
[38] D. Schwen, R.S. Averback, Intragranular Xe bubble population evolution in UO_2: a first passage Monte Carlo simulation approach, J. Nucl. Mater. 402 (no. 2–3) (2010) 116–123.
[39] C.F. Clement, M.H. Wood, The principles of nucleation theory relevant to the void swelling problem, J. Nucl. Mater. 89 (1) (1980) 1–8.
[40] M. Fell, S.M. Murphy, The nucleation and growth of gas bubbles in irradiated metals, J. Nucl. Mater. 172 (1) (1990) 1–12.
[41] S.E. Donnelly, J.H. Evans, Fundamental Aspects of Inert Gases in Solids, 1991, pp. 401–414.
[42] J.A. Turnbull, The mobility of intragranular bubbles in uranium dioxide during irradiation, J. Nucl. Mater. 62 (1976) 2–3.
[43] P. Van Uffelen, G. Pastore, V. Di Marcello, L. Luzzi, Multiscale modelling for the fission gas behaviour in the TRANSURANUS Code, Nucl. Eng. Technol. 43 (6) (2011) 477–488.
[44] L.E. Thomas, S.E. Donnelly, J.H. Evans, Condensed-phase xenon and krypton in UO_2 spent fuel, in: Fundamental Aspects of Inert Gases in Solids, 1991.
[45] K. Nogita, K. Une, High resolution TEM of high burnup UO_2 fuel, J. Nucl. Mater. 250 (no. 2–3) (1997) 244–249.
[46] T. Kogai, Modelling of fission gas release and gaseous swelling of light water reactor fuels, J. Nucl. Mater. 244 (1997) 131–140.
[47] D. Pizzocri, C. Rabiti, L. Luzzi, T. Barani, P. Van Uffelen, G. Pastore, PolyPole-1: an accurate numerical algorithm for intra-granular fission gas release, J. Nucl. Mater. 478 (Sep. 2016) 333–342.
[48] P. Garcia, et al., Nucleation and growth of intragranular defect and insoluble atom clusters in nuclear oxide fuels, Nucl. Instrum. Methods Phys. Res. Sect. B Beam Interact. Mater. Atoms 277 (2012) 98–108.
[49] M.S. Veshchunov, Modelling of grain face bubbles coalescence in irradiated UO_2 fuel, J. Nucl. Mater. 374 (no. 1–2) (2008) 44–53.